ONECENTRAL PRESS

Available online at www.onecentralpress.com

One Central Press

journal homepage: www.onecentralpress.com/functional-nanostructures

Structural, Optical and Electrical Properties of Cobalt Doped ZnO Quantum Dots

Ram Chandra Tiwari[1] and Parameswar Hari[1]*

[1]*Department of Physics and Engineering Physics, Keplinger Hall, University of Tulsa, OK, 74104*
[*]*Corresponding author*

ABSTRACT

In this study we investigated the optical and electronic properties of cobalt doped Zinc Oxide (ZnO) nanoparticles (quantum dots) fabricated by a precipitation method. We observed significant reduction in ZnO nanoparticle diameter as we increased the percentage of cobalt. UV-VIS absorption measurement show a systematic increase in bandgap from 3.40 eV to 3.69 eV as the cobalt percentage is increased from 0 to 15%. This increase in bandgap is consistent with the confinement effects observed in quantum dots. Photoluminescence studies show a blue shift in near band absorption as the cobalt doping percentage is increased from 0% to 15%. Fluorescence life time measurements of the doped and undoped ZnO samples show a reduction in radiative life time as the cobalt percentage is increased. Electrical properties of doped and undoped samples show that the series resistance in a Cole-Cole plot decreases systematically with higher doping percentage. We will discuss the quantitative changes observed in structural, optical and electrical properties of ZnO quantum dots as the doping percentage is varied from 0 -15%.

I. INTRODUCTION

Semiconductor nanoparticles have attracted lots of attention due to their applications in solar cells and medicine. For solar cell applications, composite materials made of n-type semiconductors such as ZnO, with wide band gap of the order of 3.37eV are of great interest [1]. In recent years, transition metal doped ZnO quantum dots have been extensively investigated because of their excellent chemical, mechanical, electrical, and optical properties [2, 3]. The important technological applications of quantum dots are due to the fact that their optical absorption depends on the size. The size of quantum dots in turn can be easily tuned by changing the reaction time and annealing temperature during synthesis process [4]. For ZnO quantum dots, there are two prominent emission bands observed in the photoluminescence (PL) spectrum. One band is centered in the ultra violet (UV) region, around 395 nm, and the other is centered in visible region centered at 468 nm [4]. The UV emission depends on near band radiative recombination of electron from conduction band and holes in the valence band. Since the near edge band edge direct recombination depends on the size of the band gap, it is crucially influenced by size effects due to quantum confinement [5]. On the other hand, the visible emission is thought to be related to recombination occurring via surface recombination [6].

Synthesis of ZnO nanoparticles is performed using wide range of techniques such as aqueous solution method, sol-gel method, hydrothermal method, vapor deposition method, precipitation in micro emulsions and mechanochemical processes [7]. In the present study, ZnO quantum dots were prepared by a precipitation method from Zinc acetate dihydrate and Sodium hydroxide. For cobalt doping on ZnO quantum dots, different percentage of Cobalt acetate dihydrate was used. We used precipitation method in our studies because of its several advantages over the other methods such as simplicity of deposition process, cost effectiveness, amenability to large-scale production, and the reduced need for equipment and chemicals [7].

In this work, we report an investigation of structural, optical and electronic properties of ZnO quantum dots doped with Cobalt. The properties were systematically investigated using Transmission

Electron Microscope (TEM), X-ray diffraction (XRD), UV-VIS spectrometer, photoluminescence (PL) spectrometer, fluorescence lifetime spectrometer, and L-C analyzer for performing electrical impedance spectroscopy. Further studies of optical and electronic properties of Cobalt doped ZnO quantum dots are needed to understand the changes in electronic and structural properties of QDs.

II. MATERIALS AND METHODS

Materials: The chemicals used were Zinc acetate dihydrate [$Zn(CH_3COO)_2{\cdot}2H_2O$, >99.5%], Cobalt acetate dihydrate [$Co(CH_3COO)_2{\cdot}2H_2O$, > 98%], Sodium hydroxide [NaOH, >97%] and absolute ethanol [C_2H_5OH, 99%] from Sigma Aldrich.

For the synthesis of quantum dots, 0.1M Zinc acetate was dissolved in deionized water by using magnetic stirrer in glass jars so that the particles distribute uniformly in the solution. Likewise, 0.1M solution of aqueous NaOH prepared in another jar was mixed with Zinc acetate solution drop wise at room temperature with continuous stir for 30 minutes to make homogeneous mixture and then kept at 80 °C for 2 hours. For the variation in percentage of doping, different mass of chemicals as shown in Table 1 below was used. The precipitate was washed several times using ethanol and distilled water. Cleaned precipitate was dried at 120 ^{0}C for an hour. The powder obtained from the precipitate, ZnO quantum dots, was collected and used in our studies.

For the sample preparation, the solution of ZnO quantum dots prepared in ethanol was spin coated on ITO surface, and heated at 100 ^{0}C for 5 minutes on a hot plate. This process was repeated 10 times to get the desired thickness of ZnO QDs layer. After reaching the optimum thickness the sample was annealed at 300 ^{0}C for one hour and silver paste was used as electrical contact for impedance measurement.

Characterization. The effect of cobalt doping on ZnO quantum dots on morphological, optical and electronic properties were studied using various techniques. Hitachi HF3300 transmission electron microscope was used to obtain TEM images of quantum dots. Using X-ray diffraction spectrometer size of quantum dots were measured. At room temperature, PL spectra were measured using Jasco FP6500 Spectrofluorometer with 325nm excitation wavelength. Cary 50 UV-VIS absorption spectrometer was used to measure the variation in absorption and band gap of quantum dots with change of percentage of doping. Lifetime of quantum dots were also measured using fluorescence lifetime spectrometer (LifeSpec II). Using a two probe electrical measurement unit attached to the Bode 100 vector network analyzer, one on ITO substrate and other on Quantum dots, the Cole-Cole plot was obtained for different percentage of Cobalt doping. EIS spectrum analyzer (Open source software for non-commercial use) was used to analyze the experimental data and extract the resistance and capacitance from an equivalent circuit model [8].

Table 1 Amount of Zinc acetate dihydrate and Cobalt acetate dihydrate for doping.

% of Co	Mass of Cobalt acetate (g)	Mass of Zinc acetate (g)
0	0.000	2.195
5	0.124	2.085
10	0.249	1.975
15	0.373	1.865

III. RESULTS AND DISCUSSION

The effect of doping on morphology of ZnO quantum dots with different percentage of cobalt were studied by TEM. TEM images of ZnO QDs are shown in Fig. 1. From the XRD analysis done by Cademartiri et. al. [9], they found that the XRD patterns and the results of the SEM and TEM analyses convinced them to use Debye-Scherer equation [10].

$$d = \frac{0.89\lambda}{\beta cos\theta} \quad (1)$$

Where 0.89 is Scherrer's constant, (K_α=0.154 nm) is the wavelength of X-rays, θ is the Bragg diffraction angle, and β is the full width at half-maximum (FWHM) of the diffraction peak corresponding to plane (101). While determining the average particle size of the ZnO QDs, FWHM of more intense peak corresponding to (101) plane located at 36.12° was used in Scherrer's formula. Fig. 2 shows decrease in size of the quantum dots from 27.6 nm to 12.05 nm with the increase of percentage of cobalt doping. An analysis done by Hammad et. al. [11] on X-ray diffraction reveals that the Co-doped ZnO has crystal size of 12–5 nm for 0% to 7% doping levels. On the other hand, Rongliang et.al. [12] reported that cobalt doping more than 5% doping levels in ZnO nanoparticles does not influence on the size and shape of the nanoparticles. The difference in size of the particles could be due to different preparation methods. Therefore, size of the particles is inversely proportional to the content of cobalt in quantum dots. Because of the increase in segregation at grain boundaries, size of the quantum dots decrease [13] when cobalt content increases.

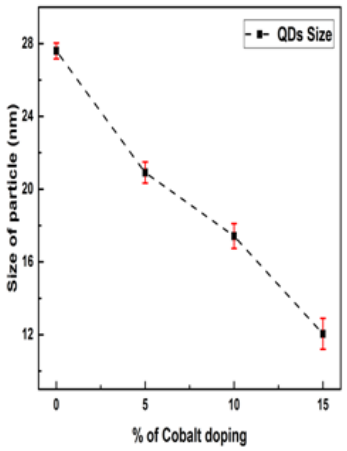

Figure 1 Variation in Size of QDs with doping.

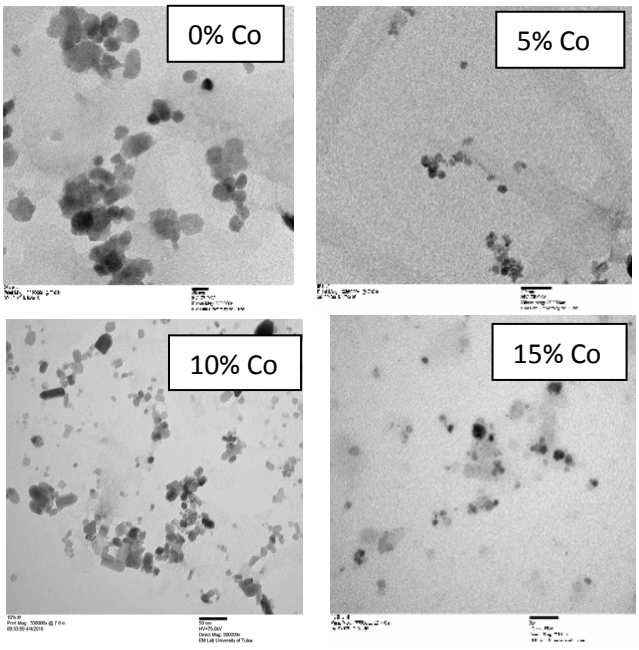

Figure 2 TEM images of cobalt doped ZnO QDs.

Structural property of QDs can also be analyzed from X-ray diffraction. Effect of cobalt doping in quantum dots can be clearly seen from the shift in position of XRD peaks. Fig. 4 shows the shifting of peak position towards lower angle (2θ) with the increase in cobalt doping. It can be seen from Fig. 3 that the intensity of diffraction peaks decreases for the increase in percentage of cobalt, which implies that dopants substituted the lattice Zn^{2+} ions [14].

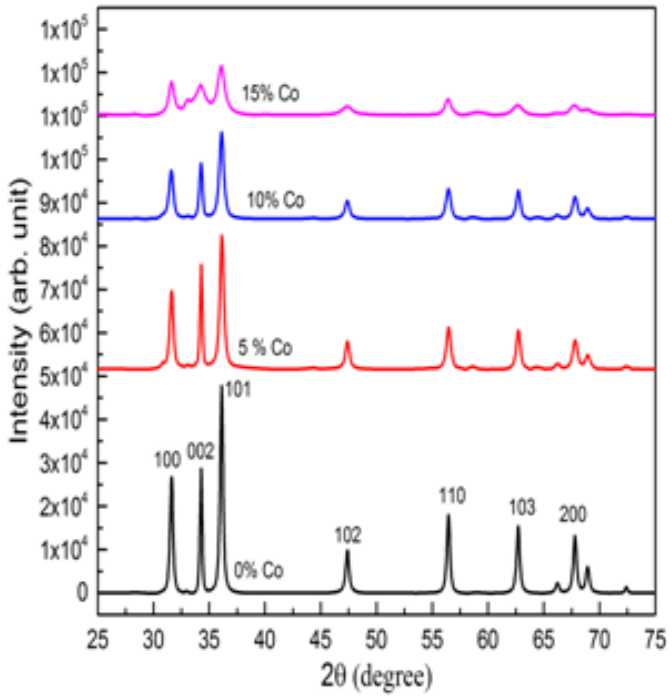

Figure 3 Powder X-ray diffraction of QDs.

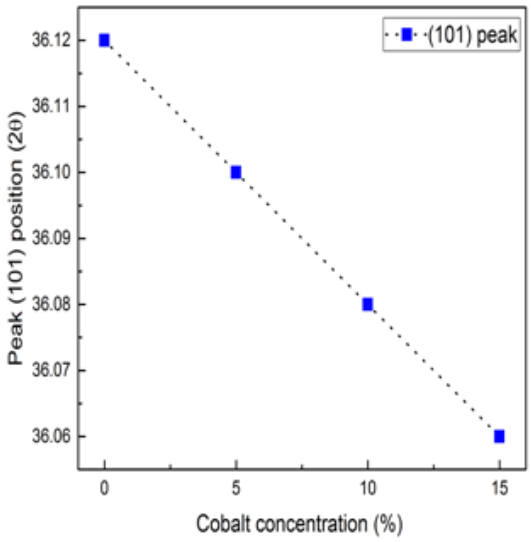

Figure 4 Shift in (101) XRD peak.

Fig. 5 depicts the UV-visible absorption spectra of quantum dots doped with 0 to 15% cobalt. From the graph, it can be seen that there was a blue shift in exciton absorption peak while increasing the cobalt content. Quantum confinement may be the reason for shift in the peak position [15]. The absorption measurement was utilized to measure the band gap using Tauc Plot equation [16]:

$$(\alpha hv)^2 = A(hv - Eg) \quad (2)$$

Where A is edge width parameter, E_g is band-gap energy and α is absorption coefficient. Fig. 6 shows the variation in band-gap energy with the change in cobalt percentage in quantum dots. The band gap energy has increased with the increase in doping level. Hammad et.al.[11] also reported that optical band gap of ZnO nanoparticles increased from 3.32 to 4.12 eV for Co doping levels from 0 to 7 %. Our investigations shows onlya small increase in band gap from 3.40 eV to 3.69 eV for doping from 0% to 15 % Co. However, small increase in bandgap in our experiment could be due to difference in preparation methods. There are many ways to support the approach for the variation in band-gap energy of quantum dots. For bulk materials, energy states are not discrete but when the size of the particles shrinks to the order of few atoms, the energy levels become discrete and due to quantum confinement bandgap increases. In addition, formula based on effective mass given below (Eqn. 3) can describe why band gap changes with doping [4, 17].

$$E^* = E_g^{bulk} + \frac{h^2}{8R^2}\left(\frac{1}{m_e^*} + \frac{1}{m_h^*}\right) - \frac{1.8e^2}{4\pi\varepsilon\varepsilon_0 R} \quad (3)$$

Where E^* is band gap, R is radius, E_g^{bulk} is the bulk band gap, m_e^* is the effective mass of the electrons,

m_h^* is the effective mass of holes in valence band of ZnO quantum dots. Equation 3 implies that band gap is inversely proportional to size (R) of the nanoparticle so band gap increases on increasing the doping percentage. From this relation we can infer that as the QD decreases in size with doping, the peak of the absorption spectrum shifts toward shorter wavelength or higher energy (Fig. 5).

Fig. 7A-E show the analysis of PL spectra in cobalt doped ZnO QDs. Fig. 7A shows the full PL spectra of cobalt doped ZnO quantum dots from 0 to 15%. There are two prominent peaks in the peaks in the PL spectra as stated earlier: one peak is present at ~395 nm and other is at ~468 nm.

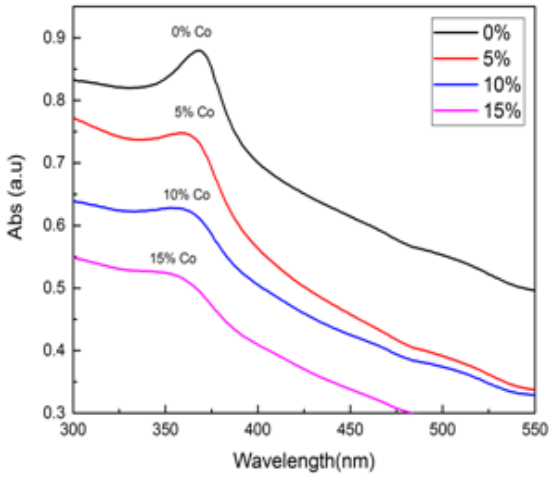

Figure 5 Absorption Spectra of cobalt doped QDs.

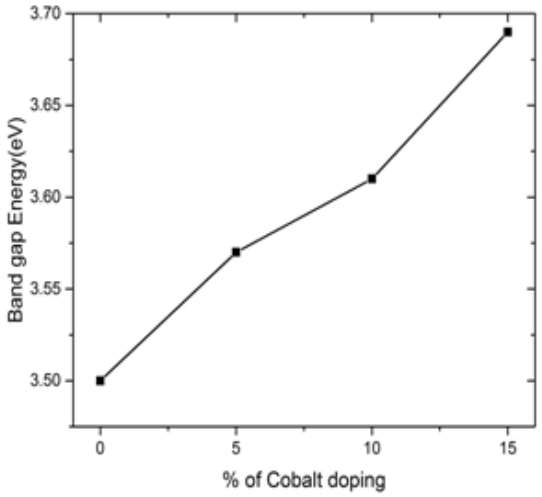

Figure 6 Variation in band gap in cobalt doped QDs.

With the increase of percentage of doping, both emission peaks showed a blue shift (Fig. 7B & D). In addition, the Full Width at Half Maximum (FWHM) (Fig. 7C & E) increased with increase in doping concentration, which could be due to several effects simultaneously present in quantum dots such as coulomb interaction, creation of vacancies and defects, and quantum size effects [15, 18, 19]. With increase in cobalt doping, particle size decreased which in turn caused more surface defects quantum dots [20, 21].

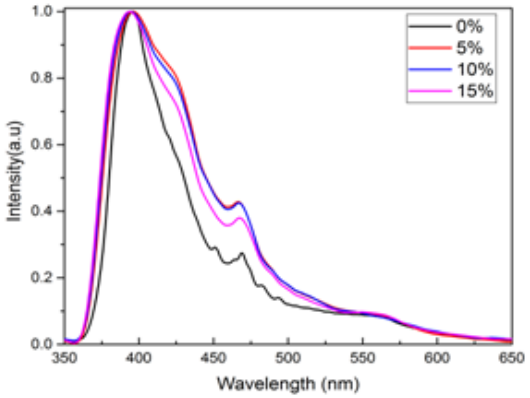

Figure 7A PL measurement of Quantum dots.

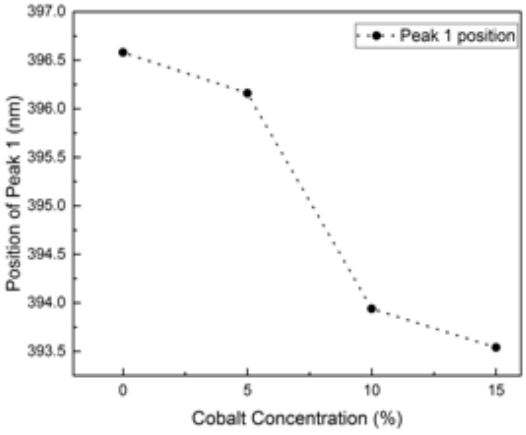

Figure 7B Position of Peak 1 of Quantum dots.

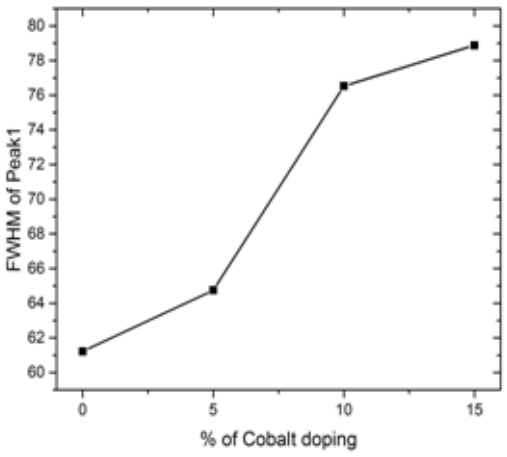

Figure 7C FWHM of Peak 1 of Quantum dots.

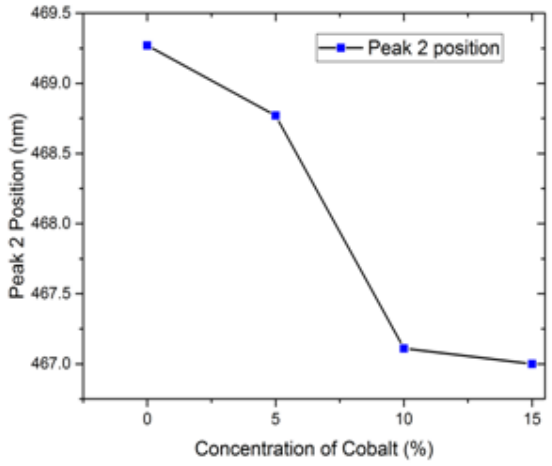

Figure 7D Position of Peak 2 of Quantum dots.

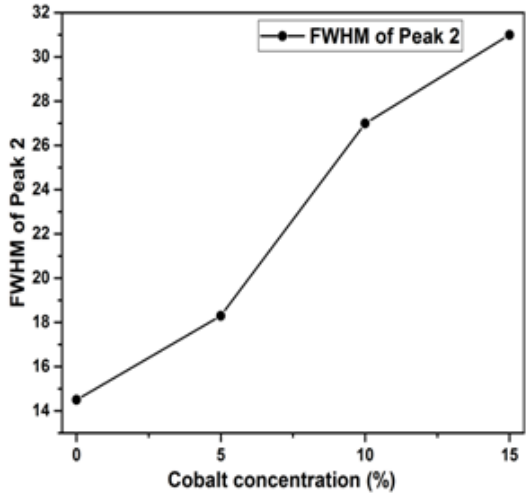

Figure 7E FWHM of Peak 2 of Quantum dots.

We further investigated changes in PL properties with cobalt doping by investigating fluorescent lifetime measurements at room temperature. Fig. 8A shows fitting of lifetime measurement of ZnO quantum dots doped with different cobalt concentrations. From Fig. 8B, it can be seen that with the increase of dopant content, lifetime decreases. The lifetime measurement results reported in this paper is in agreement with a study by Haranath et.al. [22], which found that the exciton lifetime decreased with crystal sizes, becoming shorter as the particle size decreases. Reduction in life time with the increase in cobalt doping in QDs could be attributed to increase in nonradiative transition rate via surface states [23]. Lifetime rates can be extracted by fitting the decay rates with a superposition of exponential functions as shown in Equation 4.

$$F(t) = A + b_1.exp\left(-\frac{t}{\tau_1}\right) + b_2.exp\left(-\frac{t}{\tau_2}\right) + b_3.exp\left(-\frac{t}{\tau_3}\right) \quad (4)$$

Where b_1, b_2 and b_3 are amplitudes and τ_1, τ_2 and τ_3 are the radiative decay times extracted from lifetime measurements. Fig. 8A shows a typical lifetime measurement of ZnO quantum dots doped with different proportion of cobalt using fitting Equation 3. With the increase of dopant content, the two components of lifetimes (τ_2 and τ_3) decreased as shown in Fig. 8B. The decrease in lifetime with the increase of doping may be due to decrease in ionic separation distance, which results in faster radiative decay rate than nonradiative rate [24, 25]. This effect may be also attributed to decay life time decrease in cobalt doped ZnO quantum dots.

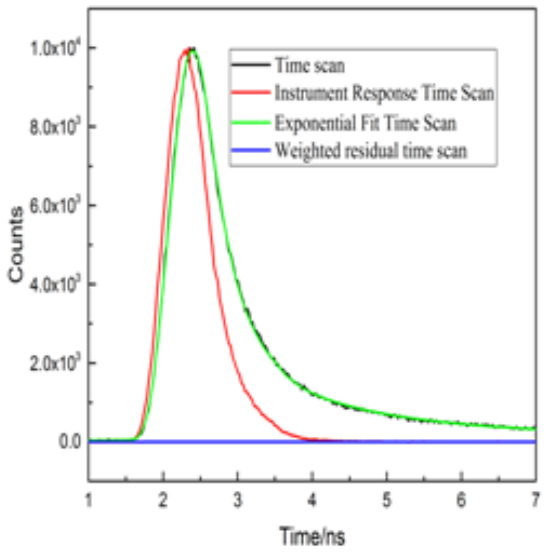

Figure 8A Fitting of lifetime measurement.

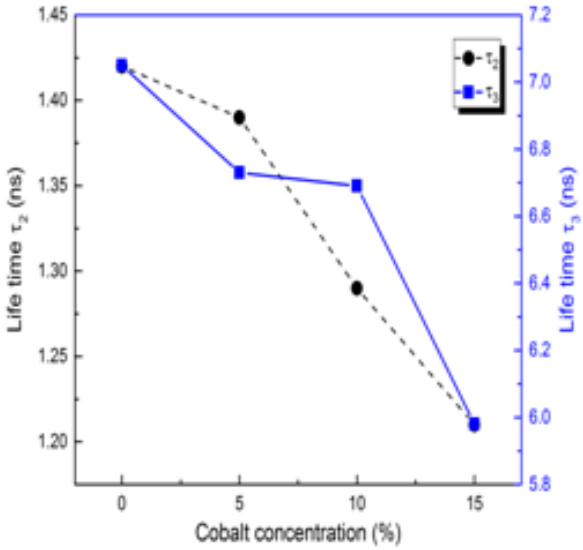

Figure 8B Life time τ_2 and τ_3 of QDs.

We investigated transport properties of doped QDs by measuring impedance analysis. Cole-Cole plot technique is a popular and powerful tool to study the electronic properties such as impedance of electrodes, grain boundary resistance and grain boundary capacitance. Impedance spectrum of

quantum dots doped from 0-15% cobalt is shown in Fig. 9A.

The Cole-Cole plot was analyzed by a RC parallel equivalent circuit model as shown in Fig. 9B. The Cole-Cole plot fitting (Fig. 9A) shows a decrease in diameter of a semicircle with the increase of cobalt content. On increasing Co doping, initially the Co atoms occupy Zn interstitial position, thus increasing the scattering from the defects. At higher doping levels the carrier concentration become much larger and the contribution from the electron concentration results in an overall decrease in electrical resistance of quantum dots [26].

Table 2 summarizes the parameters extracted from the equivalent circuit model.

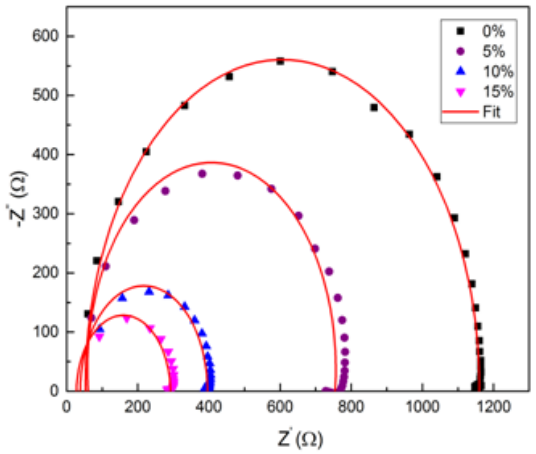

Figure 9A Cole-Cole plot of cobalt doped ZnO QDs.

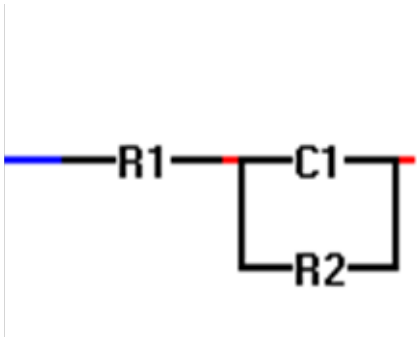

Figure 9B Equivalent circuit.

As shown in Table 2, the series resistance and effective capacitance decreases with increase in doping levels. This result is consistent with the reduction quantum dots size with doping. As the doping level increases, the size of QD decreases, and since the capacitance is directly proportional to size in a simple spherical capacitor, the capacitance of the quantum dots also decreases. Impedance measurements also show an increase in conductivity which in turn account for the decrease in resistance with increase in cobalt doping.

IV. SUMMARY

ZnO quantum dots doped with 0-15% of cobalt were successfully synthesized by a precipitation method. TEM measurement showed decrease in size of particles with increase in concentration of cobalt. Absorption peaks and photoluminescence emission spectrum peaks were found to exhibit a blue shift with increasing cobalt concentrations. This reduction in QDs size was also validated by structural measurements via X-ray. Band gap energy was found to increase with the increase of cobalt concentration in ZnO quantum dots. The changes we observe in optical and structural properties of doped ZnO QDs can be explained via enhancement in coulomb interaction, creation of vacancies, defects and quantum size effect. The fluorescence life times in quantum dots with cobalt doping were also found to decrease with increasing cobalt concentrations. This effect can be attributed to decrease in ionic separation distance with higher doping, which results in faster radiative decay rate. Finally, impedance measurements show a systematic reduction in resistance and capacitance with doping, which may be due to the enhancement in electron transport properties in quantum dots with varying doping concentrations.

V. ACKNOWLEDGEMENTS

The OK-NASA EPSCoR (project number NNX13AN01A and NNX15AM75A), TU nanotechnology and the Oklahoma Photovoltaic research institute are acknowledged for financial support. One of the authors, (RT) would like to thank Amrit Kaphle and Echo Adcock Smith for their help during this research work.

Table 2 Extraction of resistance and capacitance in doped QDs.

% of Co	Capacitance (C1) (pF)	Resistance 1 (R1) (Ohms)	Resistance 2 (R2) (Ohms)
0	28.9	75.0	1099.0
5	25.7	71.1	728.0
10	25.0	70.1	340.0
15	22.9	53.0	250.0

VI. REFERENCES

[1] V. Gandhi, R. Ganesan, H. H.A. Syedahamed, and M. Thaiyan, J. Phys Chem C.18 (2014) 9715-9725.

[2] T.V. Kolekar, H.M. Yadav, S.S. Bandgar, A. C. Raskar, S.G. Rawal, and G.M. Mishra, Nanotechnology 17, (2006) 4950–4955.

[3] S.R. Brintha, and M. Ajitha, IOSR J. Applied Chemistry, 8, 11 (2015) 66-72.

[4] L. Zhang, L. Yin, C. Wang, N. Lun, Y. Qi, and D. Xiang, *J. Phys. Chem. C*, 114, 21 (2010) 9651–9658.

[5] M. L. Kahn, Cardinal, T. Bousquet, B. Monge, M. Jubera, V. Chauret, and B. Chem, Phys Chem. 7(2006) 2392-2397.

[6] V. A. Fonoberov, and A.A Balandin, Appl. Phys. Lett. 85 (2004) 5971-5973.

[7] A. K. Radzimskaand, and T. Jesionowski, A Review Materials 7 (2014) 2833-2881.

[8] A. S. Bondarenko, and G. A Ragoisha. In Progress in Chemometrics Research, Pomerantsev A. L., Ed.; Nova Science Publishers: New York, (2005) 89–102.

[9] L. Cademartiri, E. Montanari, G. Calestani, and A. Migliori, A. Guagliardi, and G. A. Ozin, J. AM. CHEM. SOC. 128, (2006) 10337-10346.

[10] B. D. Cullity, Elements of X-Ray Diffraction, Addison-Wesley, Reading, Mass, USA, 3rd edition, (1967).

[11] T. Hammad, J. Salem, and R.Harrison, Appl Nanosci (2013) 3: 133.

[12] R. He, B. Tang, C. Ton-That, M. Phillips, and T. Tsuzuki, J. Nanopart Res (2013) 15: 2030.

[13] Zulfiqar, Y. Yuan, J. Yang, W. Wang, Z. Ye, and J. Lu, Journal of Materials Science Materials in Electronics (2016) 27:12119.

[14] V. K. Sharma, M. Najim, A.K. Srivastava, and G.D. Varma, and J. Magn. Magn. Mater. 324 (2012) 683−689.

[15] J. Zhang, S. Q. Zhao, K. Zhang, J. Q. Zhou, and Y. F. Cai. Nanoscale research Letters7 (2012) 405.

[16] M. Ghosh, and A.K. Raychaudhuri, *Nanotechnology* 18 (2007) 115618.

[17] B. Louis, J. Phys. Chem. 90, 12 (1986) 2555-2560.

[18] M.H. Huang, Y. Y. Wu, H. Feick, N. Tran, E. Weber, and P. D. Yang, *Adv Mat* 13 (2001) 113–116.

[19] M. Liu, A. H. Kitai, and P. Mascher, *J. Lumin* 54 (1992) 35–42.

[20] S. Rani, P. Suri, P.K Shishodia, and R.M. Mehra, *Sol Energy Mater Sol Cells* 92 (2008) 1639–1645.

[21] X. L. Wu, G.G. Siu, C. L. Fu, and H.C. Ong, *Appl Phys Lett* 78 (2001) 2285–2287.

[22] D Haranath, S. Sahai, A. Joshi, B. Gupta, and V Shanker, Nanotechnology 20 (2009) 425701.

[23] Z. Li, P. Wang, T. Yang, H. Yu, B. Xiao and M. Zhang,*J. Phys. Chem. C*, 119, 49 (2015) 27688–27694.

[24] P. Yuan, Y.H. Lee, M.K. Gnanasammandhan, Z. Guan, Y. Zhang, and Q.H. Xu, Nanoscale 4 (2012) 5132–5137.

[25] R. Esteban, M. Laroche, and J.J. Greffet, J. Appl. Phys. 105, 3 (2009) 033107.

[26] G. Singh, S. B. Shrivastava, and V. Ganesan. Journal of Chemical Engineering and Materials Science (2013) 1-6.